Modification of 27Cr Cast Iron with Alloying Yttrium for Enhanced Resistance to Sliding Wear in Corrosive Media

TIANCHENG ZHANG and D.Y. LI

Yttrium has been found to be beneficial to the wear resistance of (Cr, Al)-containing alloys in corrosive environments. In this study, the performance of chill-cast 27Cr white iron alloyed with yttrium during sliding wear in different media, including tap water, dilute NaOH, and HNO_3 solutions, was investigated. Compared to Y-free 27Cr cast iron, the Y-containing cast iron showed improved wear resistance. The study demonstrated that chill-cast 27Cr white iron containing 1 wt pct yttrium performed the best and that too much yttrium, however, deteriorated the material. In order to understand the beneficial role that yttrium played, mechanical properties of Y-containing and Y-free cast irons and their passive films were investigated. The electron work function, corrosion, and anodic polarization behavior of the materials were also studied. It was clarified that the beneficial role of yttrium was attributable to improved passivation capability with enhanced passive film. For comparison, sand-cast 27Cr white iron was also investigated.

I. INTRODUCTION

HIGH Cr cast iron is widely used in many fields, such as mining, oilsand, mineral processing, and construction,[1,2] *e.g.*, for slurry pumps, brick molds, coal grinding mills, shot blasting equipment, and components for quarrying, hard-rock mining, and milling.[3] The high Cr iron usually consists of hard M_7C_3 carbides and martensitic matrix (after heat treatment) or austenitic matrix (as cast).[4] Excellent wear resistance of the material results from its hard M_7C_3 carbides and tougher austenitic matrix or martensitic matrix with residual austenitic phase,[5] which is resistant to propagation of microcracks. In addition, when austenite transforms to martensite under external force, the phase transformation consumes additional deformation energy or impact energy, thus further retarding crack propagation.[6] Another merit of this material is its good corrosion resistance due to the existence of a protective passive film.[7] The high content of Cr increases the stability of the passive film, thus leading to enhanced corrosion resistance. The Cr has high passivation capability, and its anodic passivation can be established even when the surface of Cr is scratched at very high-speed.[8] Other elements have also been alloyed to high Cr cast iron to reduce the cost or to meet specific requirements.[9,10] It has been observed that yttrium addition can further improve the strength of cast iron[11] and its corrosion resistance.[12] Recent studies have shown that yttrium addition can also markedly diminish corrosive wear. Liu and Li[13] demonstrated that the corrosive wear of stainless steel and aluminum alloys in a mixture of lubricant and sulfuric acid can be decreased by adding a small amount of yttrium powder to the lubricant containing the acid. The present authors have also observed that yttrium is very beneficial to the resistance of stainless steel and aluminide coatings to wear in different corrosive media.[14,15] The improved performance of the passive alloys is largely attributed to the enhancement of their passive films when yttrium is added.[16] It is expected that yttrium may also play the same role when alloyed into high-Cr cast white iron, a widely used industrial wear-resistant material.

In this work, the performance of 27Cr-cast white iron alloyed with yttrium during sliding wear in various corrosive solutions was evaluated, in comparison with Y-free cast 27Cr iron. Mechanical, physical, and electrochemical properties of passive films on the Y-containing and Y-free cast irons were investigated using a nanomechanical probe, a scanning Kelvin probe, and an electrochemical system.

II. EXPERIMENTAL PROCEDURE

The chill-cast white iron used for the present study contained the following elements (wt pct): Cr 26.8, C 2.89, Mn 1.25, Ni 0.52, Si 0.42, P 0.04, S 0.04, balanced by Fe. 0.5 pct Y, 1 pct Y, and 1.5 pct Y were, respectively, alloyed to the cast iron to make Y-containing cast iron samples. Chill-cast ingots were made using an electric arc furnace with a water-cooled copper hearth in argon atmosphere. Pin samples having a cross-section area of 5×8 mm for wear test were machined from the chill-cast ingots. Samples of $8 \times 8 \times 8$ mm were also prepared for corrosion, scratch, indentation, and polarization experiments, respectively. These samples were mounted with epoxy resin. For comparison, a sand-cast 27Cr cast iron was also evaluated. Before the tests, all samples were mechanically ground with emery paper up to 600 grit and then polished to an average roughness (R_a) of 0.03 μm. Vickers hardness of the samples was determined using a microhardness tester (Newage Testing Instruments, Inc., Indianapolis, IN, USA).

Sliding wear test was performed on a pin-on-disc tester. The counter disc, 150 mm in diameter and 2 mm in thickness, was made of commercial 420 stainless steel and was mounted in a container so that the wear test could be performed in a corrosive solution. During the test, a target pin sample slid on the disc at a sliding speed of 0.6 m/s over a sliding distance of 5 Km. Tap water, 0.01 mol/l NaOH (pH 12), and 0.001 mol/l HNO_3 (pH 3) solutions were selected

TIANCHENG ZHANG, Postdoctoral Fellow, and D.Y. LI, Associate Professor, are with the Department of Chemical and Materials Engineering, University of Alberta, Edmonton, AB, Canada T6G 2G6. Contact e-mail: dongyang.li@ualberta.ca

Manuscript submitted May 14, 2001.

as three kinds of corrosive media. Corrosive wear resistance of the pin sample was evaluated by measuring its weight loss after sliding against the steel disc over 5 km. The normal load exerted on the pin sample was kept at 40 N.

A Gamry framework, commercial-corrosion measurement system was used for potentiodynamic polarization test. The scan rate was 0.33 mV/s. A saturated calomel electrode and a piece of platinum were used as the reference and auxiliary electrodes, respectively. The steady-state corrosion rate of a sample was determined by measuring the weight loss of the sample after being immersed in a corrosive solution for 168 hours at room temperature.

In order to evaluate passive films on the samples, a universal microtribometer (Center for Tribology, Inc., Mountain View, CA, USA) was used to evaluate the resistance of the passive films to scratch and indentation on a microscale. The samples for the tests were passivated under a potential of 0.5 V above the corrosion potential in different corrosion media for 6 hours. The tip was a pyramidal tungsten carbide. During the microscratch and microindentation tests, the tip moved horizontally and vertically, respectively, under a force that was increased linearly from 0 to a designed level. The velocity of the tip was 0.02 mm/s, and the durations of indentation and scratch were 30 and 120 seconds, respectively. Failure of a passive film during microindentation or microscratch test was determined by monitoring variations in the electrical contact resistance between the indenter tip and the target sample surface.

Mechanical properties of thin passive films on the tested samples were investigated using a nanomechanical probe (Hysitron Inc., Minneapolis, MN, USA).[17] During nanoindentation, a diamond indenter tip penetrated into a passive film under a light normal load that was increased continuously up to 100 μN, and the load was then gradually decreased back to zero. The corresponding load to indentation depth curve was recorded. The ratio (η) of the recoverable deformation energy to the total deformation energy is a measure of the contribution of elasticity to deformation.[18] η can be calculated using the following equation:

$$\eta = \frac{W_d}{W_r} \qquad [1]$$

where W_d is the area under the loading curve from zero to maximum load, and W_r is the area under the unloading curve from maximum load to zero. The indentation depth reflects the hardness of the passive film.

A scanning Kelvin probing system was used to measure the electron work functions of passive films on different samples. Figure 1 shows a schematic of the scanning Kelvin probe system. The host PC communicated with three subsystems: (1) a digital oscillator, (2) a 16-bit digital to analog converter, and (3) sample translation (*x*, *y*, and course *z*) *via* the parallel interface. The vibrating probe assembly consisted of a voice-coil housing containing the voice-coil driver element, magnets and two 25-mm-diameter stainless-steel springs. A sinusoidal waveform was applied to the voice coil to control the frequency (173.5 Hz) and amplitude (174 μm) of oscillation of the probe tip. The mean distance between the probe tip and the sample surface was 600 ± 10 μm. The probe tip was made of gold with 0.5 mm in diameter, which was directly mounted onto an I/V converter (current-to-voltage). The sample and probe are connected

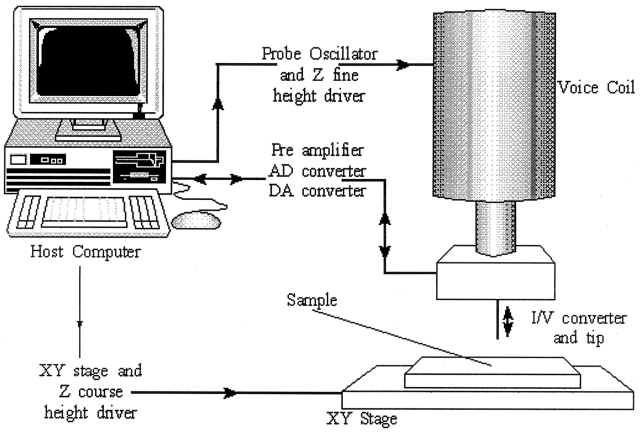

Fig. 1—Schematic illustration of a scanning Kelvin probe system.

via a voltage source termed the "backing potential" (V_b = 5 V), which was controlled by a preamplifier. The average peak-to-peak value (V_{ptp}) over 50 cycles with respect to the applied potential (5 V) was determined by a data acquisition system. The fractional changes in the capacity and, thus, the electron work functions were determined from the obtained data. Before the test, the sample surface was potentiostatically passivated at 0.5 V above the corrosion potential for 6 hours.

III. RESULTS

A. *Microstructure*

Microstructures of various cast iron samples are illustrated in Figure 2. The sand-cast 27Cr iron was either hypoeutectic or eutectic. During solidification, its liquidus reaction was:

$$\text{Liquid} \rightarrow \text{primary austenite} + \text{eutectic}$$

The followed solidus eutectic reaction at about 1275 °C was:

$$\text{Solid} \rightarrow \text{eutectic } M_7C_3 \text{ carbides} + \text{austenite}$$

The matrix was austensite, which could partly decompose during cooling in the sand mould with the reaction:

$$\text{Saturated austenite} \rightarrow \text{secondary carbides} + \text{martensite} + \text{retained unsaturated austenite}$$

The decomposition reaction was both time and temperature dependent. On cooling at approximately 1050 °C, the secondary carbides started to precipitate out of the austensite and ended at about 750 °C. When slowly cooled to room temperature, the unsaturated austenite partially transformed to martensite. As a result, the sand-cast iron mainly consisted of a martensitic matrix with residual austensite (marked by A in Figure 2(a)) and eutectic M_7C_3 carbides (marked by B in Figure 2(a)). For the chill-cast 27Cr iron, the structure was much finer than the sand-cast structure. There was little or no formation of the secondary carbides during rapid cooling and the matrix consisted mostly of retained austenite (mark by C in Figure 2(b)) and finer eutectic carbide (marked by D in Figure 2(b)). Finer microstructure was observed when the chill-cast 27Cr iron was alloyed with yttrium (Figure 2(c)). The yttrium addition might act as an inoculant for nucleation of eutectic carbides, thus leading to finer

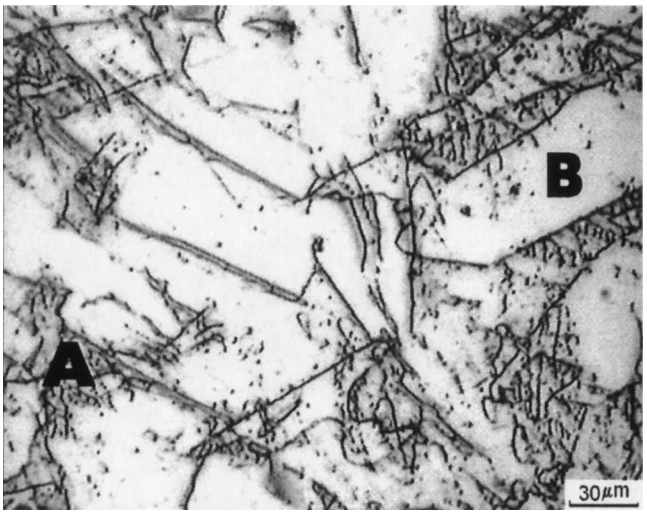

(*a*)

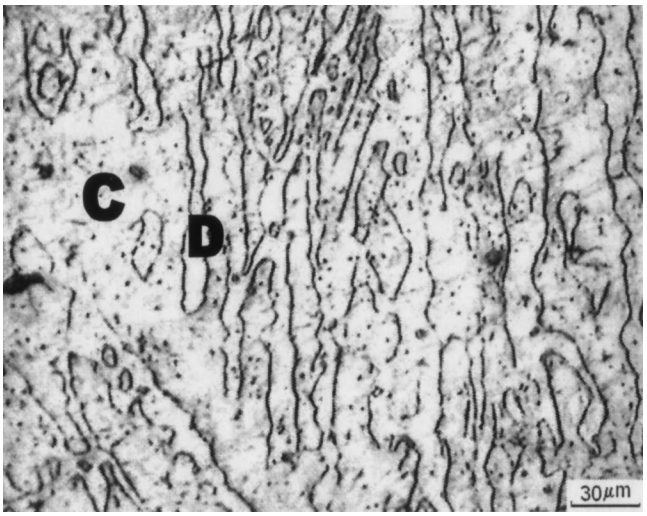

(*b*)

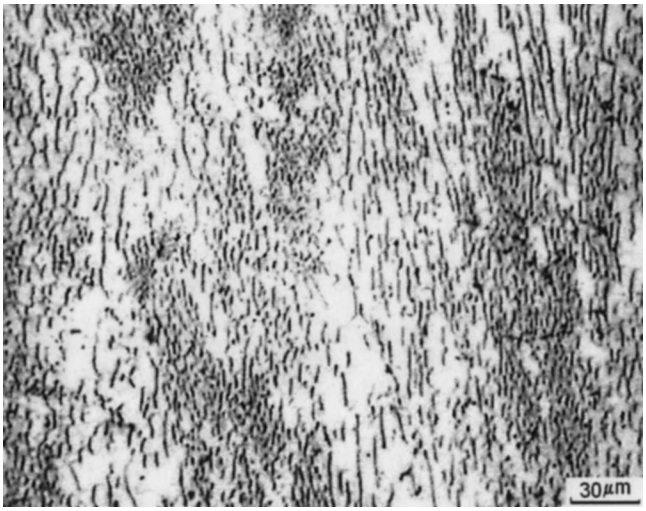

(*c*)

Fig. 2—Microstructures of Y-free and Y-containing samples: (*a*) sand-cast 27 Cr iron, (*b*) chill-cast 27 Cr iron, and (*c*) 1 pct Y-containing chill-cast 27 Cr iron.

microstructure. The form of yttrium in the cast iron samples was not clear because the amount of yttrium was not enough to be detected using available X-ray diffractometer or the energy dispersive X-ray spectroscopy. According to a phase diagram of the Fe-Y binary system,[19] the Fe-Y alloy mainly consists of α-Fe and $Fe_{17}Y_2$ phase when the content of yttrium is less than 10 wt pct. The solubility of yttrium in γ-Fe is less than 1.29 wt pct at the eutectic temperature[20], and should be lower at room temperature. Further studies on microstructure are being conducted using transmission electron microscopy.

B. *Effects of Y on Corrosion Behavior of the Cast Iron*

In order to evaluate effects of the alloyed yttrium on the wear behavior of 27Cr cast iron in corrosive environments, steady corrosion rates of 27Cr cast-iron samples with and without yttrium were determined by measuring their weight losses after being immersed in corrosive solutions for 168 hours. Steady-state corrosion rates of samples in tap water, dilute NaOH and HNO_3 solutions were presented in Figures 3(a), (b), and (c), respectively. Each corrosion rate was obtained by averaging results of three measurements. It is clear that yttrium improved the corrosion resistance of 27Cr cast iron in all the tested solutions. The 1 wt pct yttrium-containing iron exhibited the highest corrosion resistance, and the sand-cast iron showed the lowest corrosion resistance in all three kinds of media. In both tap water and the HNO_3 solution, a small amount of light yellow corrosion product was observed on the sand-cast iron surface and in the solutions as well. Similar product was found on the chill-cast iron surface when corroded in the HNO_3 solution.

Potentiodynamic polarization tests were carried out for further information on the corrosion resistance of the samples. Figure 4(a) illustrates potentiodynamic polarization curves of various samples in tap water. The Y-free and Y-containing chill-cast iron show passivation characteristic, while the sand-cast iron showed poor polarization behavior in tap water. One may clearly see that yttrium improved the polarization behavior of the chill-cast iron. As demonstrated, yttrium addition increased the corrosion potential (E_{corr}) and decreased the current density in the passivation region (i_p).

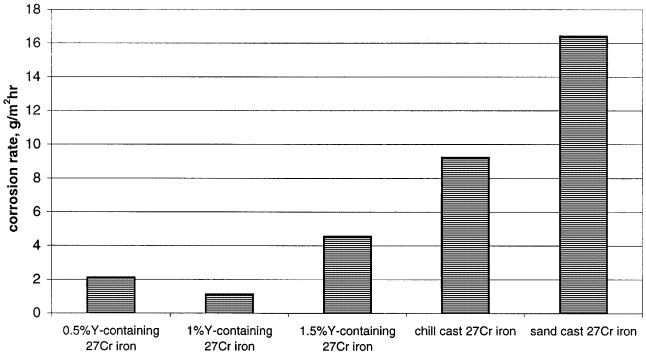

(*a*)

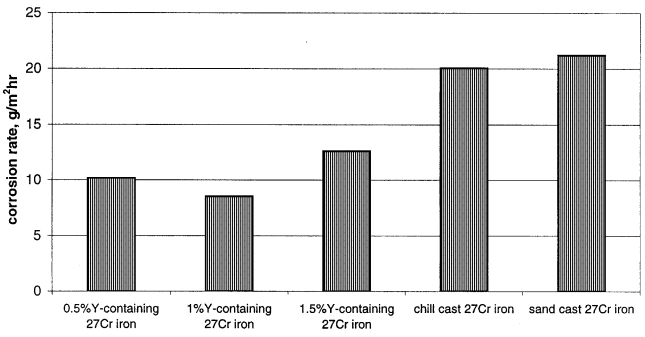

(*b*)

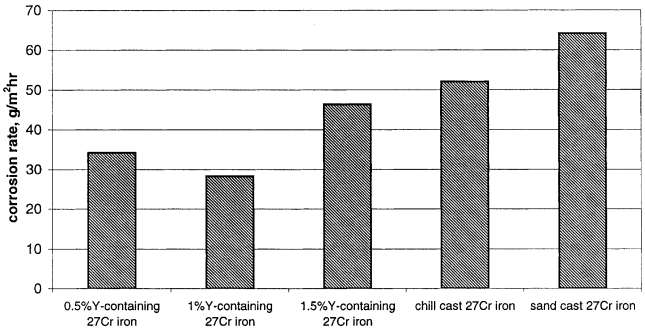

(*c*)

Fig. 3—Corrosion rates of the materials: (*a*) corrosion rates in tap water, (*b*) corrosion rates in NaOH (pH 12) solution, and (*c*) corrosion rates in HNO_3 (pH 3) solution.

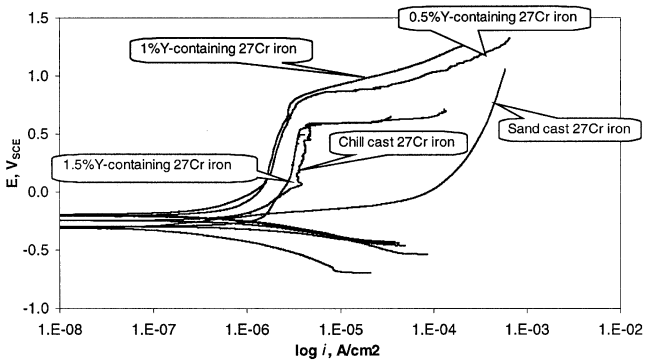

(*a*)

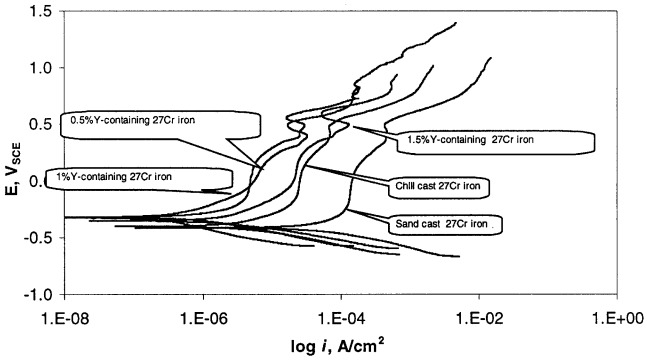

(*b*)

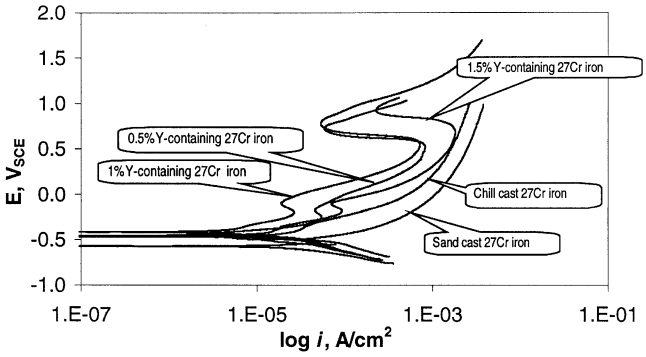

(*c*)

Fig. 4—Polarization curves of the materials in different media: (*a*) polarization behavior of the materials in tap water, (*b*) polarization behavior of the materials in NaOH (pH12) solution, and (*c*) polarization behavior of the materials in HNO_3 (pH3) solution.

The cast iron containing 1 pct yttrium performed the best. In the case of the NaOH solution (pH 12), as illustrated in Figure 4(b), all tested materials were passivated. Similar to corrosion in tap water, the yttrium addition increased E_{corr} and decreased i_p. In comparison with their polarization behavior in tap water (Figure 4(a)), the materials generally had lower corrosion potentials and higher current densities within the passive region in the NaOH solution. Polarization curves of the materials in the HNO_3 (pH 3) solution are illustrated in Figure 4(c). In this solution, the materials showed the lowest corrosion potentials and the highest anodic dissolution current densities, and especially, the Y-free cast irons exhibited poorer anodic polarization behavior. Again, yttrium improved the polarization behavior of the cast iron in this particular medium. The results of the polarization test are consistent with the result of corrosion rate measurement presented in Figure 3.

C. *Effects of Yttrium on the Mechanical Behavior of the Cast Iron and its Passive Film*

It was demonstrated in our previous work on 304 stainless steel[14] that a small amount of yttrium almost had no influence on mechanical properties of 304 stainless steel, but its passive film was considerably enhanced. In the present study, effects of yttrium on passive film of the cast iron were investigated using microindentation and microscratch techniques. During the tests, changes in the surface electrical contact resistance (ECR) as a function of applied load was *in situ* monitored with respect to time. Since the passive film is an oxide, its electrical resistance is significantly larger than that of metals. When the passive film was broken down during microindentation or microscratch by a tungsten carbide tip, the electrical contact resistance dropped steeply.

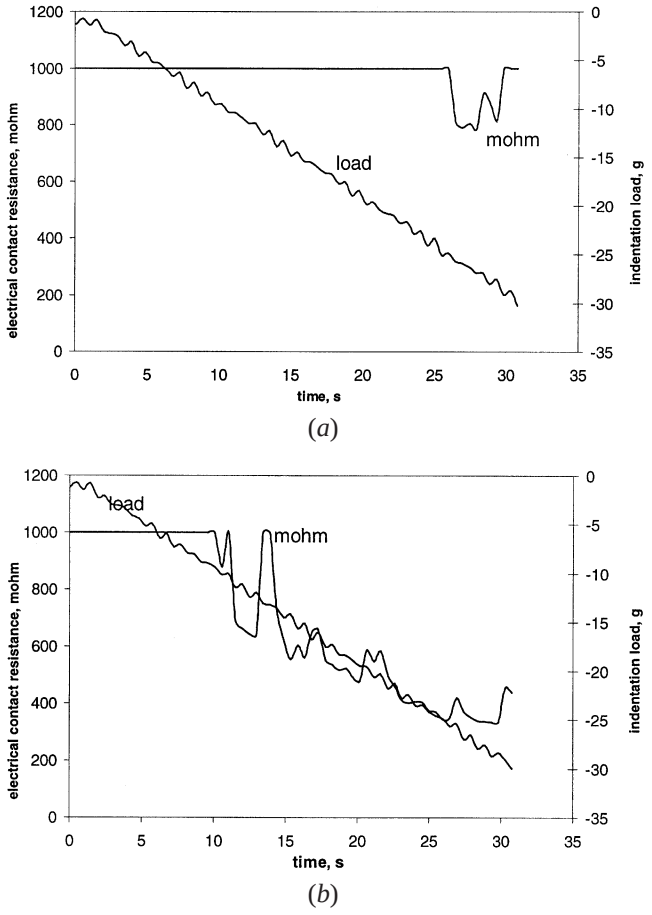

Fig. 5—Typical microindentation curves of Y-free and 1.0 pct Y-containing chill-cast 27Cr iron after passivation in NaOH (pH 12) solution: (*a*) indentation of 1.0 pct Y-containing 27Cr iron after passivation in NaOH (pH 12) solution, and (*b*) indentation of chill-cast 27Cr iron after passivation in NaOH (pH 12) solution.

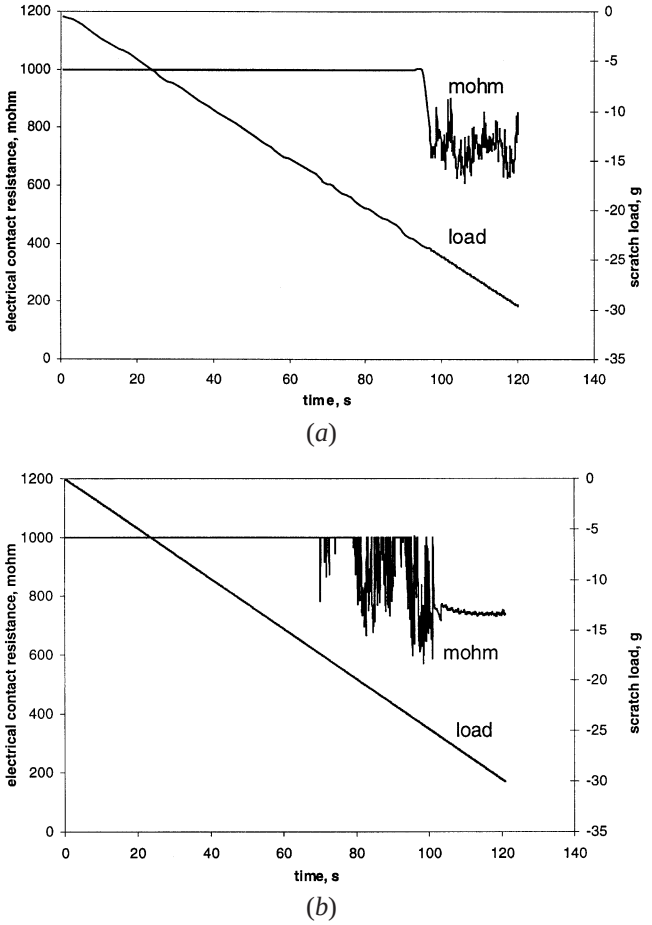

Fig. 6—Typical microscratch curves of Y-free and 1.0 pct Y-containing chill cast 27Cr iron after passivation in NaOH (pH 12) solution: (*a*) scratch of 1.0 pct Y-containing 27Cr iron after passivation in NaOH (pH 12) solution, and (*b*) scratch of chill-cast 27Cr iron after passivation in NaOH (pH 12) solution.

The critical normal load corresponding to the drop in the ECR reflected the load-carrying capability of the passive film. Typical indentation and scratch curves are presented in Figures 5 and 6, respectively. Two curves in each figure represent changes in the applied normal load and the contact electric resistance (CER), respectively, with respect to time. As the applied load was increased and reached a critical value, the ECR suddenly dropped, as Figures 5 and 6 illustrated. The critical loads corresponding to the drop of CER during indentation and scratch were presented in Table I. Under the same condition, alloyed yttrium increased the load-carrying capability of the passive film and the critical load of 1 pct yttrium-containing iron was the highest. However, too much yttrium, *e.g.*, 1.5 wt pct, decreased the load-carrying capability. In the absence of yttrium, the passive film on the chill-cast 27Cr iron showed higher load-carrying capability than that of the passive film on the sand-cast 27Cr iron.

In order to check the yttrium-modified mechanical properties of bulk cast iron, Vickers hardness of Y-free and Y-containing samples was determined by averaging five measurements for each sample. All samples showed nearly identical values of hardness equal to Hv567 $\pm$ 5, except the sand-cast 27Cr iron, which was harder (Hv625 $\pm$ 5). The hardness measurement indicated that the yttrium addition did not influence the hardness of the cast 27Cr irons. The higher hardness of the sand cast may result from its higher fraction

Table I. Critical Loads Corresponding to the Drop of the CER

		Critical Load (g)	
Material	Medium	Indentation	Scratch Test
0.5 pct Y-containing iron	water	20.63	23.14
	NaOH	15.68	20.72
	HNO_3	14.15	13.54
1 pct Y-containing iron	water	25.70	28.32
	NaOH	25.97	23.14
	HNO_3	18.82	19.78
1.5 pct Y-containing iron	water	18.66	14.81
	NaOH	9.29	13.62
	HNO_3	4.91	12.05
Chill-cast iron	water	18.34	19.55
	NaOH	10.18	17.43
	HNO_3	8.54	12.62
Sand-cast iron	water	12.16	13.0
	NaOH	4.87	10.74
	HNO_3	3.49	10.13

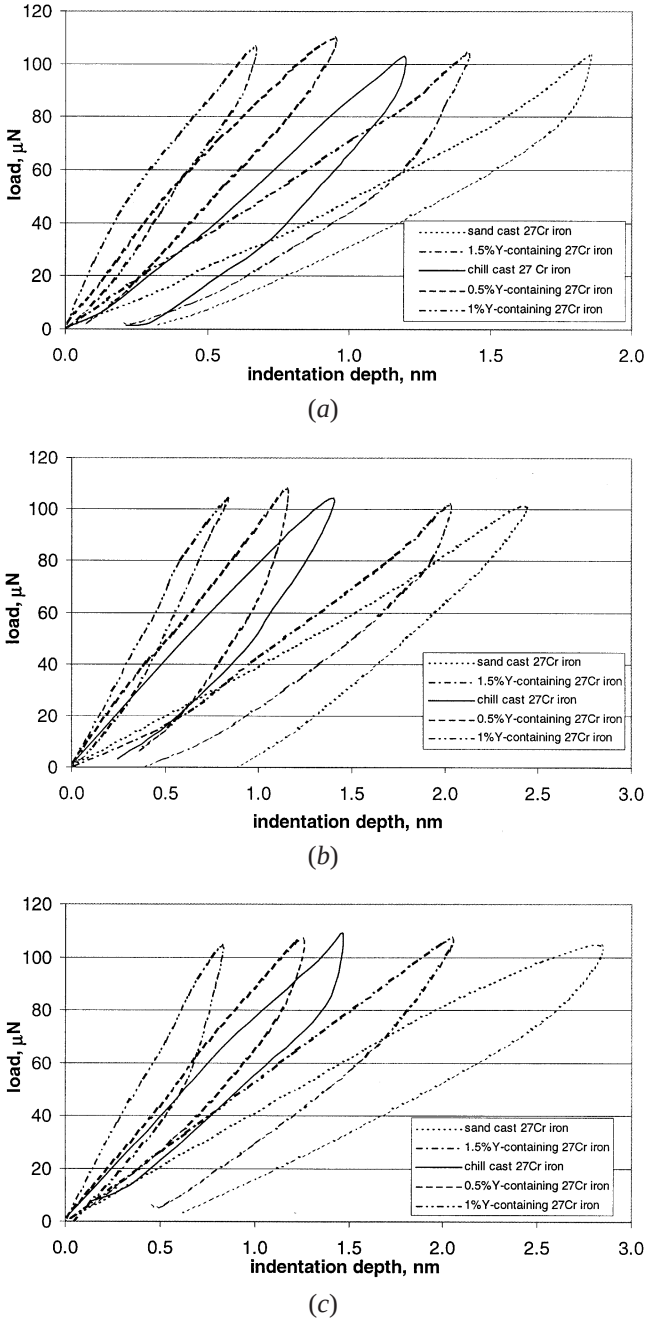

Fig. 7—Nanoindentation curves of the materials after passivation in the corrosive media: (*a*) nanoindentation curves of the materials after passivation in tap water, (*b*) nanoindentation curves of the materials after passivation in NaOH solution, and (*c*) nanoindentation curves of the materials after passivation in HNO_3 solution.

of martensitic phase. Mechanical behavior of thin passive films on the Y-free and Y-containing samples was also investigated. It was difficult to determine hardness of the passive films using a conventional method, since the passive films were too thin with their thickness generally in the range of 10^0 to 10^1 nm. A nanomechanical probe was thus employed to determine the mechanical behavior of a passive film on a nanometer level.

Figure 7 presents load vs indentation depth curves of the samples after passivation treatment in the corrosive media. The maximum normal load for the nanonindentation test was 100 μN. The maximum indentation depth and the ratio of the recoverable deformation energy to the total deformation energy (η) were presented in Table II. Although the indentation curves were not very smooth at this load level, the mechanical behavior of the passive films can be clearly reflected by these curves. The hardness was closely related to the maximum indentation depth; the harder a film, the smaller was its indentation depth. As illustrated in Figure 7, the indentation depths of all samples were less than 3 nm. Therefore, the influence from the substrate on the indentation behavior of a passive film could be largely minimized. From Table II, one may see that yttrium addition increased both the hardness and η value of the passive film. One percent yttrium appeared to be the optimum quantity and resulted in superior mechanical properties, compared to others. The 1.5 pct yttrium addition, however, deteriorated the passive film. The passive film formed on the sand-cast 27Cr iron was the softest and the least elastic due to its largest maximum indentation depth and lowest η value (Table II).

Table II. Mechanical Properties of Passive Films Obtained by Nanoindentation Test

Media	Materials	Maximum Depth (nm)	η (Pct)
Tap water	0.5 pct Y-containing iron	0.95	76
	1 pct Y-containing iron	0.70	83
	1.5 pct Y-containing iron	1.50	69
	chill-cast iron	1.25	70
	sand-cast iron	1.80	68
NaOH	0.5 pct Y-containing iron	1.20	62
	1 pct Y-containing iron	0.80	78
	1.5 pct Y-containing iron	2.00	62
	chill-cast iron	1.40	63
	sand-cast iron	2.40	54
HNO_3	0.5 pct Y-containing iron	1.25	73
	1 pct Y-containing iron	0.71	74
	1.5 pct Y-containing iron	2.05	67
	chill-cast iron	1.48	68
	sand-cast iron	2.80	60

D. *Effects of Yttrium on the Electron Work Function of Passivated Samples*

The Kelvin probing technique has been used to measure corrosion potentials, to study the mechanism of corrosion, to investigate interfacial failure, and to explore passivation phenomena.[21,22,23] Using this technique, the electron work function (EWF) of a material can be determined, which reflects the ability of an electron to escape from the Fermi surface of a material and become a free electron. Because the formation and dissolution of a passive film involve electron transfer, the EWF could, therefore, be a measure of the electrochemical stability or inertness of the passive film. Figure 8 shows a typical distribution of the EWF of different samples after passivation treatment in an HNO_3 solution. The average EWF value of each material is illustrated in Figure 9. For the same material, the EWF of its passive film was the highest after passivation in tap water and the lowest after passivation in the HNO_3 solution. The passive film on the sand-cast 27Cr iron had lower EWF, compared to that on the chill cast. This implies that the passive film on the

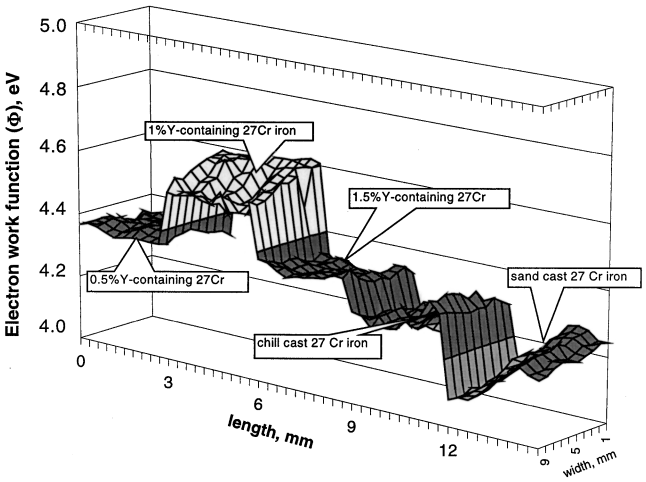

Fig. 8—The distribution of the electron work function of passive films on different samples after passivation treatment in tap water.

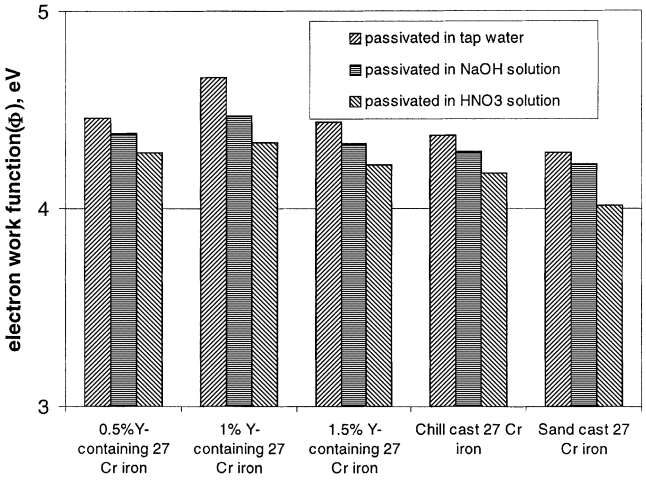

Fig. 9—Average values of the electron work functions of the passive films on different samples.

sand-cast iron was less stable or less resistant to electrochemical attack than that on the chill-cast iron. Alloying yttrium apparently increased EWF of the passive film formed on the chill-cast 27Cr iron (*e.g.*, by 0.33 eV for the 1 pct Y cast in the case of passivation in tap water). The EWF measurement is consistent with both the corrosion test (Figure 3) and the polarization experiment (Figure 4). Since the passive film may contain Y_2O_3,[24] this oxide phase might be responsible for the difference in EWF between the passive film of Y-containing sample and that of Y-free one.

E. *Effects of Y on Corrosive Wear Resistance of the Cast Iron*

Corrosive wear resistance of Y-free and Y-containing samples was evaluated using a pin-on-disc wear tester. Weight losses of the tested samples in tap water, NaOH solution, and HNO_3 solution are presented in Figures 10(a), (b), and (c), respectively. All samples had the lowest wear loss when worn in tap water, moderate wear loss in the NaOH solution, and the highest wear loss in the HNO_3 solution. It was

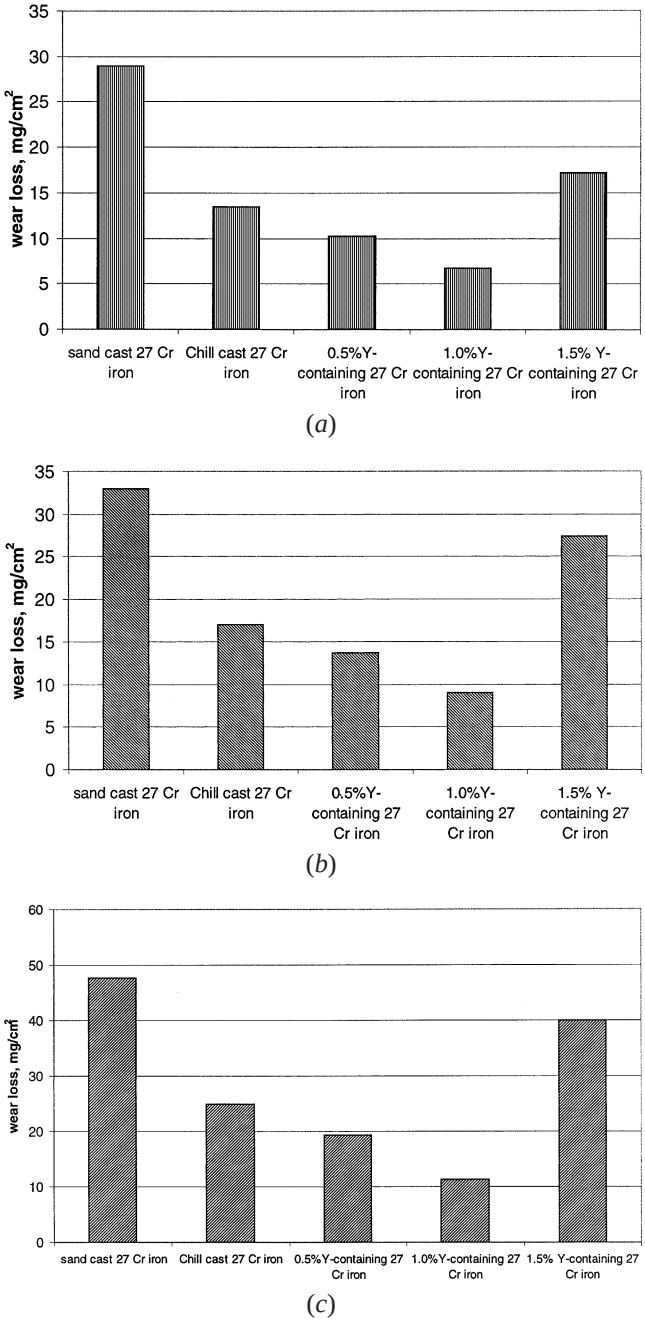

Fig. 10—Corrosive wear behavior of the tested materials: (*a*) corrosive wear in tap water, (*b*) corrosive wear in the NaOH solution, and (*c*) corrosive wear in the HNO_3 solution.

demonstrated that alloying with yttrium significantly diminished the wear loss of 27Cr chill-cast iron. However, too much yttrium deteriorated the material. As demonstrated, when the nominal content of yttrium was 1.5 wt pct, the wear resistance of the cast 27Cr iron was considerably decreased and was inferior to that of the Y-free chill-cast iron sample.

IV. DISCUSSION ON POSSIBLE MECHANISM RESPONSIBLE FOR THE BENEFICIAL EFFECT OF YTTRIUM

The resistance of a material to wear and corrosion is strongly affected by its microstructure and corresponding

mechanical and electrochemical properties. It is known that high-Cr white cast iron has eutectic carbides (M_7C_3) in a matrix that may consist of austenite, pearlite, bainite, and martensite.[4] Chill casting suppresses the transformation of austenite to martensite as well as the growth of carbide particles, thus leading to finer microstructure containing more austenite and finer carbides (Figure 2(b)). During sand casting, however, the austenite may partially transform to martensite (possibly with some pearlite) with bigger carbide particles (Figure 2(a)) due to lower cooling rate. As a result, the chill-cast iron is relatively softer (due to lower fraction of martensite) but more corrosion resistant than the sand-cast iron (as shown in Figures 3 and 4) due to its less microstructural inhomogeneity. In general, the wear resistance of a material increases with its hardness. The hardest sand-cast iron, however, performed the worst during wear in the corrosive media even in tap water, as illustrated in Figure 10. This happened largely due to the lowest corrosion resistance of the sand-cast iron, which showed the poorest polarization behavior in all the tested media. The coarser microstructure of sand-cast iron consisting of martensite, residual austenite, and carbides accelerated galvanic corrosion.

When yttrium was added, no difference in hardness was observed between the Y-containing and Y-free chill-cast iron samples. However, yttrium improved the cast iron against wear in all the corrosive media (Figure 10). As Figure 4 illustrates, the yttrium addition improved the anodic passivation behavior and corrosion resistance of the chill-cast iron at different levels, depending on the amount of yttrium. This improvement certainly benefited from the improvement of the mechanical behavior of the passive film on Y-containing samples with enhanced load-carrying capability against indentation and scratching (Tables I and II). The enhancement of the passive film may result from possible formation of Y_2O_3 phase in the film,[24] which may strengthen the passive film. Yttrium could also enhance the adherence of the passive film to the substrate. Tien and Pettit[25] investigated the interfacial bonding between a FeCrA alloy and its oxide scale. They observed that the adherence of the oxide scale was considerably improved when a small amount of yttrium or scandium was added to the alloy. The increase in the interfacial bonding could be attributed to the possible role of the oxygen-active elements in (a) acting as vacancy sinks to reduce interfacial vacancies, (b) enhancing the atomic bonds across the oxide film-substrate interface, and (c) developing oxide pegs penetrating into the grain boundaries.[25,26,27] The situation could be similar for the passive film-substrate interface. The enhanced scratch resistance of the passive film on Y-containing samples may result from both the improvement in mechanical behavior and probable enhancement of the interfacial bonding strength. A more adherent and stronger passive film provides more protection to the surface against electrochemical and mechanical attacks.

In addition to the preceding benefit of yttrium to the passive film, yttrium may also be beneficial to intrinsic electrochemical properties of the cast iron and thus its polarization behavior with increased corrosion potential (E_{corr}) and decreased i_p.

The improvement in the mechanical properties of the passive film due to the existence of yttrium should be responsible for the increase in the resistance of the cast iron to corrosive wear to a large degree, bearing in mind that yttrium showed little influence on hardness of the bulk materials. Under the synergistic attack of corrosion and wear, the performance of passive film could become more important. This may be seen from the following analysis. The results of the nanoindentation test (Table II) showed that 1.5 pct Y weakened the passive film with larger maximum d and lower η value. No matter how and why this happened, the deterioration of the passive film, associated with decrease in its resistance to scratch and indentation, resulted in a decrease in the resistance of the cast iron to corrosive wear (Figure 10). The load-carrying capability and scratch resistance of the passive film are of importance to the resistance of the cast iron to corrosive wear. By comparing Y-free chill cast to that containing 1.5 pct Y, one may notice that the former had a higher corrosion rate, but its passive film was stronger than that on the later. As a result of the improvement in its passive film's mechanical properties, the former showed a relatively higher resistance to corrosive wear. In our previous work on 304 stainless steel,[16] it has also been confirmed that a small amount of yttrium addition is remarkably beneficial to corrosive wear of the material through enhancing its passive film.

V. CONCLUSIONS

Research was carried out to investigate effects of alloying yttrium on the resistance of cast 27Cr iron to wear in three corrosive media, including tap water, dilute NaOH solution (pH = 12), and HNO3 solution (pH = 3), respectively. The following is the summary of the results obtained in this study.

1. The chill-cast 27Cr iron had lower corrosion rate than the sand-cast iron in the tested media. This difference could be attributed to coarser microstructure of the sand cast that consisted of more martensite and coarser carbides.
2. Alloying yttrium into the chill-cast 27Cr iron increased its corrosion resistance in the given media at different levels, varying with the amount of yttrium.
3. The 1 wt pct yttrium turned out to be the optimal quantity that was considerably beneficial to the corrosive wear resistance of the material in all tested media. It was demonstrated that the alloyed yttrium markedly improved the mechanical properties and the failure resistance of the passive film on the cast iron.
4. Too much yttrium deteriorated the cast iron with inferior passive film and resulted in poor performance of the cast iron during wear in the corrosive media.

ACKNOWLEDGMENTS

The authors are grateful for the financial support from the Alberta Science and Research Authority (ASRA).

REFERENCES

1. W. Fairhurst and K. Rohrig: *Foundry Trade J.*, 1974, vol. 30, pp. 685-98.

2. J. Dodd and J.L. Parks: *Met. Forum*, 1980, vol. 3, pp. 3-27.
3. J.R. Davis: *ASM Specialty Handbook, Cast Irons*, ASM INTERNATIONAL, Materials Park, OH, 1996, p. 111.
4. F. Maratary and R. Usseglio-Nanot: *Transformation Characteristics of Chromium and Molybdenum White Irons*, Climax Molybdenum S.A., Paris, 1971.
5. K.H. Zum Gahr: *Metall. Trans. A*, 1980, vol. 11A, pp. 613-20.
6. J. Dodd and J.L. Parks: *Int. Cast Met. J.*, 1980, vol. 5, pp. 47-54.
7. B. Baroux: in *Passivity of Metals and Semiconductors*, M. Froment, ed., Elsevier, Amsterdam, 1983, pp. 531-43.
8. N.D. Tomashov and L.P. Vershinina: *Electrochim Acta*, 1970, vol. 15, pp. 501-07.
9. D.M. Stefanescu and S. Cracium: *Fonderic*, 1977, vol. 32, pp. 51-60.
10. G.J. Cox: *Foundry Trade J.*, 1974, vol. 10, pp. 31-38.
11. A.A. Anikin, K.L. Vlaskina, and E.I. Gurevich: *Izv. V.U.Z. Chernaya Metall.*, 1984, vol. 7, pp. 112-15.
12. A.A. Anikin, V.M. Zhivaikin, A.G. Zhukov, N.N. Kireev, and V.A. Khotinskii: *Izv. V.U.Z. Chernaya Metall.*, 1982, vol. 8, pp. 87-89.
13. R. Liu and D.Y. Li: *Wear*, 1999, vols. 225–229, pp. 968-74.
14. T.C. Zhang, and D.Y. Li: *Mater. Sci. Technol.*, 1999, vol. 15, pp. 1441-446.
15. T.C. Zhang and D.Y. Li: *Surface Coatings Technol.*, 2000, vol. 130, pp. 57-63.
16. X.Y. Wang and D.Y. Li: *Mater. Sci. Eng. A*, 2001, A315, pp. 158-165.
17. *Hysitron Nanomechanical Test Instrument User's Manual*, Hysitron Inc., Minneapolis, MN, USA, Sept 10, 1996.
18. R. Liu, D.Y. Li, Y.S. Xie, R. Liewellyn, and H.M. Hawthorne: *Scripta Mater.*, 1999, vol. 41, pp. 691-96.
19. *Binary Alloy Phase Diagrams*, vol. 2, edited by Thaddeus B. Massalski, American Society for Metals, Metals Park, Ohio, 1986.
20. O. Kubaschewski: in *Iron-Binary Phase Diagrams*, Springer-Verlag, New York, NY, 1982, pp. 168-70.
21. M. Stratmann, R. Feser, and A. Leng: *Electrochim. Acta*, 1994, vol. 39, pp. 1207-14.
22. A. Leng and M. Stratmann: *Corr. Sci.*, 1993, vol. 34, pp. 1657-83.
23. L.T. Han and F. Mansfeld: *Corr. Sci.*, 1997, vol. 39, pp. 119-202.
24. E. Caudron, H. Buseail, R. Cueff, Y.P. Jacob, and M.F. Stroosnijder: *Thin Solid Films*, 1999, vol. 350, pp. 168-72.
25. J.K. Tien and F.S. Pettit: *Metall. Trans.*, 1972, vol. 3, p. 1587.
26. J.E. McDonald and J.G. Eberhart: *Trans. TMS-AIME*, 1965, vol. 223, p. 512.
27. E.J. Felten: *J. Electrochem. Soc.*, 1961, vol. 108, p. 490.